Helium atom line-intensity ratios as an integrated diagnostic tool for low-pressure and low-density plasmas

Akira Ueda, Taiichi Shikama 🆔, Tatsuya Teramoto, Takanori Higashi, Yohei Iida, and Masahiro Hasuo

View Online **Export Citation** **CrossMark**

ARTICLES YOU MAY BE INTERESTED IN

Helium atom line-intensity ratios as an integrated diagnostic tool for low-pressure and low-density plasmas

Akira Ueda,[1] Taiichi Shikama,[1,a)] Tatsuya Teramoto,[1] Takanori Higashi,[1] Yohei Iida,[2] and Masahiro Hasuo[1]

[1]*Department of Mechanical Engineering and Science, Graduate School of Engineering, Kyoto University, Kyoto 615-8540, Japan*
[2]*Bunkoukeiki Co., Ltd., Hachioji, Tokyo 192-0033, Japan*

The intensity ratios between specific pairs of helium atom (HeI) emission lines are functions of the electron temperature (T_e) and density (n_e), and these functions have been used for the analysis of T_e and n_e in various types of discharge plasma. We applied this method to a low-density ($n_e < 10^{18}$ m^{-3}) plasma, where the procedure of the analysis is markedly different from that of higher-density plasmas. The 2^1S and 2^3S metastable atom densities are affected by transport, making it practically necessary to set T_e, n_e, the metastable atom densities, and the optical escape factors, which represent the effect of photoexcitation, as unknown variables and determine them simultaneously. Conversely, the transport of metastable atoms can be evaluated from the analysis. *Published by AIP Publishing.*
https://doi.org/10.1063/1.5027167

Low-pressure helium discharge plasmas having relatively low electron densities of $n_e < 10^{18}$ m^{-3} are widely used in glow, capacitively coupled, inductively coupled, and electron cyclotron resonance (ECR) discharges, and they are also found in the edge region of higher density discharges. For the measurement of T_e and n_e in these plasmas, the Langmuir probe and Thomson scattering are the most common techniques. However, in addition to these techniques, a spectroscopic method using HeI line-intensity ratios is becoming a viable alternative owing to the recent improvements in its measurement accuracy for various types of plasma, e.g., Refs. [1–7]. The method can measure not only T_e and n_e but also the metastable and ground-state atomic densities. The former is essential in atom lithography,[8,9] stimulated desorption,[10] and the removal of hydrocarbon contaminants,[11] and the latter is necessary to evaluate the ionization degree[12] and the depletion[13] and dynamics[14] of neutrals. The method is thus usable as an integrated diagnostic for discharges.

When applying this method to low-density plasmas, extra care should be taken in the analysis compared with the case of high-density plasmas. In this study, we present the detailed procedure for the analysis using a helium ECR discharge plasma and discuss the validity of the obtained parameters. The procedure is the basis of our previously reported application.[12] Note that we use the term "low-pressure" in the sense that the effect of neutral collisions is negligible in the excitation and de-excitation of atoms.

This method is based on the collisional-radiative (CR) modeling of helium atoms. The CR model solves the equations of continuity for atoms in their excited states, which are written as

$$\frac{\partial n_p}{\partial t} + \nabla \cdot (n_p \boldsymbol{v}_p) = \sum_{q<p} C_{qp} n_e n_q$$
$$+ \sum_{q>p} (F_{qp} n_e + \Lambda_{qp} A_{qp}) n_q + (\alpha_p n_e + \beta_p + \gamma_p) n_e n_z$$
$$- \left[\left(\sum_{q<p} F_{pq} + \sum_{q>p} C_{pq} + S_p \right) n_e + \sum_{q<p} \Lambda_{pq} A_{pq} \right] n_p, \quad (1)$$

where n_p is the density of excited atoms in state p, $\boldsymbol{v}_p$ is the mean velocity, and n_z is the He$^+$ ion density. C, F, S, α, β, and γ are the rate coefficients of electron-impact excitation, de-excitation, ionization, three-body recombination, radiative recombination, and dielectric recombination, respectively, A is the spontaneous emission coefficient, and Λ is called the Biberman–Holstein coefficient or optical escape factor (OEF),[15–17] which represents the effective reduction in A due to radiation trapping. The first and second subscripts on the variables denote the initial and final states of the reactions, respectively.

When the magnitude of the convection term is sufficiently smaller than that of the annihilation term, the left-hand-side of Eq. (1) can be approximated to zero, i.e., the quasi-steady-state (QSS) approximation.[18] However, atoms in the two metastable states, 2^1S and 2^3S, have a long radiative lifetime and generally do not satisfy this condition in low-density plasmas. The QSS approximation is thus usually applicable to states except for the ground and metastable states, and then Eq. (1) is solved as

$$n_p = r_p^0 n_e n_z + r_p^1 n_e n_{1^1\mathrm{S}} + r_p^2 n_e n_{2^1\mathrm{S}} + r_p^3 n_e n_{2^3\mathrm{S}}, \quad (2)$$

where r_p^0, r_p^1, r_p^2, and r_p^3 are called population coefficients, $n_{1^1\mathrm{S}}$ is the ground-state density, and $n_{2^1\mathrm{S}}$ and $n_{2^3\mathrm{S}}$ are the 2^1S and 2^3S metastable-state densities, respectively. On the right-hand side, the terms from left to right represent the production of excited atoms from He$^+$ ions, ground-state atoms,

a)Electronic mail: shikama@me.kyoto-u.ac.jp

2^1S metastable atoms, and 2^3S metastable atoms. We consider only ionizing plasmas and neglect the first term.

For most plasmas in use, the effect of radiation trapping becomes significant only for the resonant $1^1S - n^1P$ transitions associated with the ground state[2,7] owing to its large lower-state density. Since most of the lines used for the measurement belong to $n = 2$–3 and 2–4 transitions, where n is the principal quantum number, we practically consider OEFs only for the 1^1S–3^1P and 1^1S–4^1P transitions, which we denote as Λ_{3^1P} and Λ_{4^1P}, respectively. The variation of the densities in the $n = 3$ and 4 states as a result of the increases in the n^1P-state densities ($n = 2$ and $n > 4$) due to radiation trapping is small.[2] The unknown parameters are thus T_e, n_e, Λ_{3^1P}, Λ_{4^1P}, n_{1^1S}, n_{2^1S}, and n_{2^3S}.

T_e and n_e can be determined by comparison of the calculated n_p with values measured from the intensities of HeI lines. The determination procedure relies on the facts that C_{qp} for singlet and triplet states have different dependences on T_e, the relative densities of excited states change with n_e, the magnitude of Λ locally changes the upper-state density of the transition, n_{2^1S} and n_{2^3S} selectively affect the singlet- and triplet-state densities, respectively, and n_{1^1S} determines the contribution of the excitation from the ground-state relative to that from the metastable states.

In high-density plasmas, the QSS approximation becomes valid even for metastable states; thus, the total number of unknown parameters is reduced to ≤ 4, i.e., T_e, n_e, Λ_{3^1P}, and Λ_{4^1P}, where n_{1^1S} is omitted when analyzing the density ratio. When radiation trapping is negligible, two excited-state density ratios, n_{3^3S}/n_{3^3S} and n_{3^1D}/n_{3^1S}, are usually used to evaluate T_e and n_e, respectively,[19] where the subscripts represent the electronic states. When radiation trapping is not negligible, Λ_{3^1P} and Λ_{4^1P} can be determined by measuring two additional excited-state densities.[2]

In low-density plasmas, it is necessary to determine all six parameters, which is the main difference from the case of high-density plasmas. A standard procedure is to measure as many excited-state densities as possible and simultaneously determine all the unknown parameters by least-squares fitting of the calculated densities to the measured values.[3,4,7,12]

We performed experiments using a helium ECR discharge plasma.[12] Briefly, the plasma was produced using 2.45 GHz and 0.8 kW microwaves in a simple cusp field. The shape of the resonance layer was a spheroid with major and minor axes of 168 and 92 mm, respectively. Figure 1 is a schematic illustration of the device and its cross section at the midplane. We define the $r\theta z$ coordinate system as shown in the figure. Measurements were performed at a helium pressure of 23 mPa at the vacuum chamber. The emission was collected using a collimated viewing chord in the $r\theta$-plane at $z = 12$ mm and transmitted via an optical fiber to a wide-wavelength-range spectrometer (B&W Tek BTC112E; 200–900 nm wavelength range and 1.2 nm wavelength resolution at 546 nm). The viewing chord was terminated by a viewing dump to reduce the effect of reflection, and the intensities of the measured spectra were absolutely calibrated using a standard tungsten-halogen lamp taking into account the transmittance of the window.
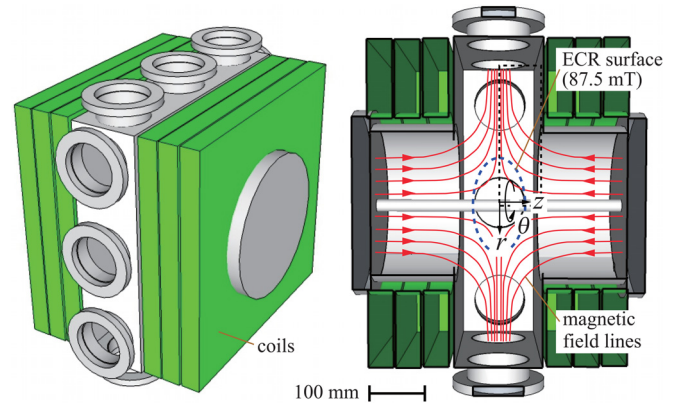

FIG. 1. Schematic drawing of ECR discharge device: overall view (left) and cross section at the midplane (right).

Chord-integrated spectra were measured while varying the distance between the viewing chord and the z-axis. A spectrum is shown in Fig. 2. In addition to HeI lines, we identified HeII ($n = 3$–4), CII, and HI ($n = 2$–3, 4, and 5) lines. We carefully checked the superposition of impurity and unidentified lines on HeI lines and excluded possibly contaminated HeI lines from the analysis. Consequently, the ten lines indicated in the figure were used. The chord-integrated intensity and its standard deviation were then evaluated from the area of the least-squares-fitted Gaussian function for the HeI and HeII lines. Since all the observed transitions are optically thin, their intensities were converted to local emissivities $\varepsilon_{pq}(r)$ using the Abel inversion while taking into account the numerical error.[12] The upper-state density $n_p(r)$ was then calculated from the relation $\varepsilon_{pq}(r) = (h\nu_{pq}/4\pi)n_p(r)A_{pq}$, where h is Planck's constant and ν_{pq} is the transition frequency. The results are shown in Fig. 3. The standard deviations of these data increase toward the center of the device owing to the accumulation of the error.

We used a CR model source code developed by Goto[20] and implemented a nonlinear least-squares fitting procedure with Λ_{3^1P} and Λ_{4^1P} as auxiliary input parameters. The densities in the $n = 3$ and 4 states calculated using the model were
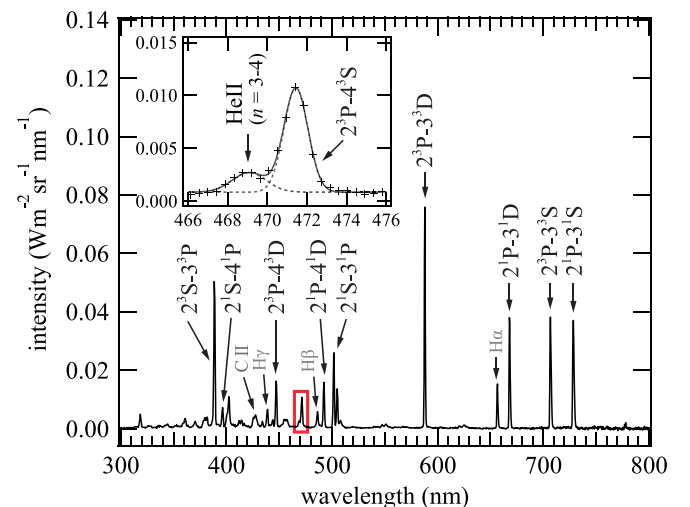

FIG. 2. Spectrum measured on a viewing chord at a distance of 56 mm from the z-axis. The inset shows an enlarged spectrum around 471 nm and fitting curves.
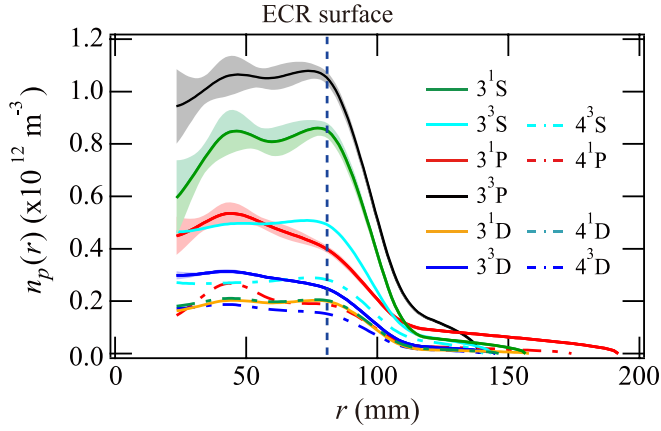
FIG. 3. Radial distributions of $n_p(r)$. The shaded areas indicate the error bars for the 3^1S, 3^1P, 3^3P, and 3^3D states as examples. For the other states, the error bars are omitted for better visibility.

least-squares fitted to the measured values using the input parameters as fitting variables and weighting the residues with the inverse standard deviations of $n_p(r)$. The results are shown in Fig. 4. The adopted fitting procedure gives a smaller reduced chi-square value[23] than procedures with a reduced number of parameters.[12] Also, comparative studies using similar fitting procedures and Langmuir probes were conducted in high-[4] and low-density[7] plasmas with T_e ≤ 10 eV, and both showed agreement between the two methods almost within the measurement error. A comparison with other diagnostics at higher T_e is required.
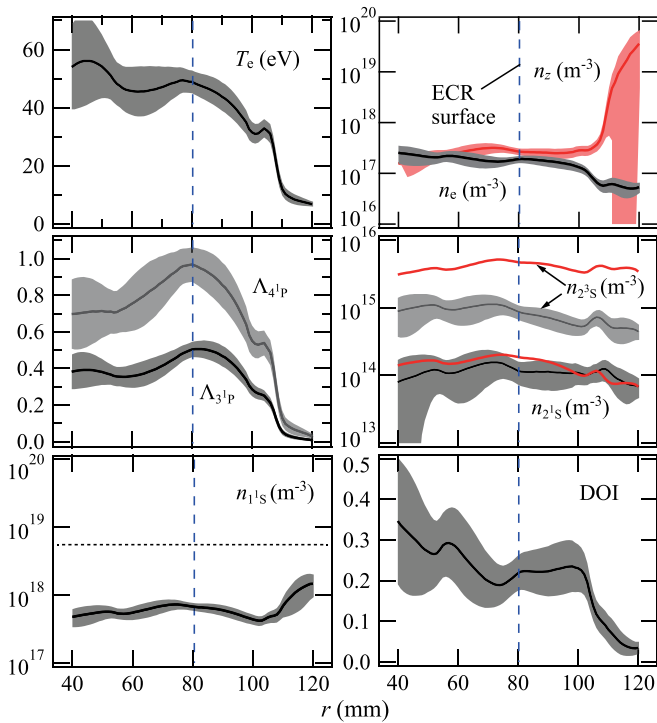
The accuracy of the determined n_{1^1S} mainly depends on those of the evaluated emissivities. The result appears to be reasonable since in the edge region it tends to approach the density evaluated from the pressure of 23 mPa and room temperature of 300 K at the vacuum chamber ($r = 240$ mm). We have not yet identified the mechanism for the decrease in n_{1^1S} inside the plasma, but the effects of ionization and increased atomic temperature were suggested in preceding studies on argon ECR plasmas in diverging magnetic fields.[21,22] Below, we discuss the effects of the other parameters on T_e and n_e.

The effect of radiation trapping increases in the edge region with the decrease in the emissivity since the magnitude of the absorption relative to that of the emission increases owing to the strong irradiation from the inner region. This tendency can be confirmed in Fig. 4 from the significant decrease in Λ in the edge region. The larger values of Λ in the inner region ($r \leq 60$ mm) than those previously measured at 67 mPa[12] are due to the variation of the radial profile of the emissivity. This also suggests that the radial profiles of the plasma parameters are considerably different under the two pressure conditions. If we omit this effect from the analysis, the increased densities of the 3^1P and 4^1P states due to the absorption are mainly compensated for by increasing T_e and decreasing n_{2^1S}. For the former, the electron-impact excitations to the singlet states are relatively increased compared with those to the triplet states with increasing T_e when $T_e \geq$ 20 eV (see inset of Fig. 5). However, the densities of not only the 3^1P and 4^1P states but also the other singlet states are increased, and this effect is mitigated by decreasing n_{2^1S}. We also found that n_e and n_{1^1S} slightly change to enable further compensation. Thus, the primary consequence is the overestimation of T_e. The increase was by 30% at $r = 80$ mm and fourfold at 110 mm from the values in Fig. 4. If the target plasma has a simpler geometry, such as a cylinder or a slab, the OEF can be calculated from first principles.[15–17] The errors in the OEFs can then be reduced, but if the magnetic field strength
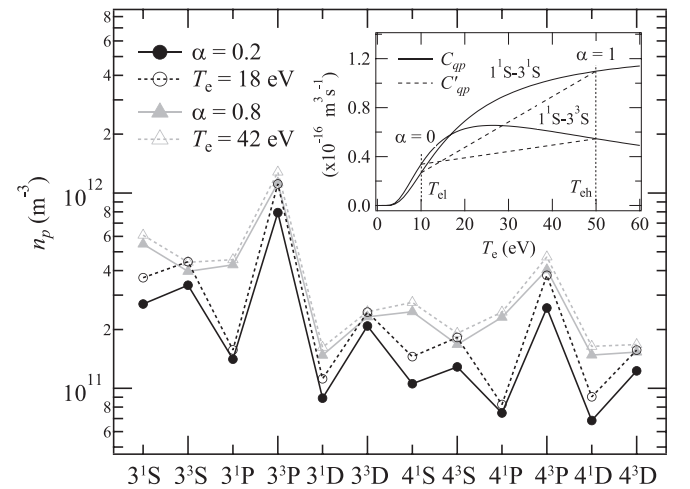

FIG. 4. Radial distributions of the evaluated plasma parameters. n_{2^1S} and n_{2^3S} obtained under the QSS approximation are shown by red lines. The degree of ionization (DOI) is defined as $n_e/(n_e + n_{1^1S})$. The horizontal dotted line corresponds to the density calculated using the pressure measured at the vacuum chamber (23 mPa) at room temperature (300 K).

FIG. 5. Calculated n_p in the case of two electron temperatures (solid lines with $T_{el} = 10$ eV and $T_{eh} = 50$ eV) and one temperature corresponding to $T_{e(avg)}$ (dotted lines). The other parameters were fixed to $n_e = 1 \times 10^{17}$ m^{-3}, $\Lambda_{3^1P} = 0.3$, $\Lambda_{4^1P} = 0.5$, $n_{1^1S} = 1 \times 10^{18}$ m^{-3}, $n_{2^1S} = 2 \times 10^{14}$ m^{-3}, and $n_{2^3S} = 2 \times 10^{15}$ m^{-3}. The inset shows C_{qp} and C'_{qp} for the $1^1S - 3^1S$ and $1^1S - 3^3S$ excitations.

exceeds ~ 0.1 T, the Zeeman effect, which reduces the absorption, should be considered.[24,25]

If we enforce the QSS approximation even for the metastable states, T_e and n_e will be changed for the same reason as in the above discussion, namely, the decrease/increase in the densities in the singlet and triplet states are compensated for by changing T_e and then n_e. In Fig. 4, n_{2^1S} and n_{2^3S} obtained under the QSS approximation are plotted by red lines; the other parameters were fixed to the originally determined values. n_{2^3S} is approximately three times larger than that without the QSS approximation, indicating that the convection term in Eq. (1) is not negligible. n_{2^3S} obtained without the QSS approximation is smaller in the entire radial range; thus, it is inferred that the convection is mainly in the axial (z) direction. Meanwhile, the value of n_{2^1S} obtained with and without the QSS approximation are comparable. This is because the magnitude of the annihilation term, which is dominated by the excitations to the adjacent upper states, is larger for the 2^1S state than for the 2^3S state. If we assume the QSS approximation only for the 2^1S state from the beginning, the changes in T_e and n_e are less than 20% from the values in Fig. 4.

The relative magnitudes of the convection terms to the annihilation terms are approximately 0.6 and 4 for the 2^1S and 2^3S states, respectively. Since the annihilation term is proportional to n_e, a value of n_e roughly sevenfold that under the present conditions, i.e., $n_e \gtrsim 10^{18}$ m^{-3}, is required to satisfy the QSS approximation for the 2^3S state. However, in a discharge with an increased neutral pressure, justification of the QSS approximation at smaller n_e is expected, since the convection is reduced owing to the smaller mean free path of elastic collisions with the ground-state atoms.

n_e is determined by the relative densities of all the excited states included in the fitting, and thus the effects of radiation trapping and the metastable densities are smaller than those in the case of determining T_e. In our data, the variation is within a factor of two for all possible combinations of the fitting, namely, with and without the radiation trapping and the QSS approximation.

We confirmed the validity of the evaluated n_e using the value of n_z estimated from the emissivity of the HeII $n = 3$–4 line and corona model analysis.[18] The ion species of the present plasma is dominated by He$^+$; thus, the charge neutrality requires the condition $n_e \simeq n_z$. The ground-state He$^+$ ion density can then be obtained from the relation

$$n_z = \frac{4\pi\epsilon_{43}}{h\nu_{43}n_e C_{14}} \frac{\sum\limits_{q<4} A_{4q}}{A_{43}}, \qquad (3)$$

where ϵ_{43} and ν_{43} are the emissivity and frequency of the HeII line, respectively. The other variables are related to He$^+$ ions: A_{4q} is the A-coefficient of the $n = q - 4$ transition, and C_{14} is the electron-impact excitation rate coefficient from the ground state ($n = 1$) to the upper state. The data of A_{4q} and C_{14} were taken from NIST and NIFS databases, respectively. The evaluated n_z plotted in Fig. 4 is in good agreement with n_e in the region $r < 100$ mm.

The excitation-emission processes of hydrogen-like ions are analogous to those of hydrogen atoms when replacing T_e

and n_e with T_e/Z^2 and n_e/Z^7, respectively, where Z is the nuclear charge of the ions.[26] T_e/Z^2 and n_e/Z^7 are ~ 10 eV and $\sim 10^{15}$ m^{-3}, respectively, and the excitation-emission process of hydrogen atoms with these parameters can be approximated by the corona model.[26] This is, however, not the case in the edge region owing to the decrease in T_e. The observed increase in n_z at $r > 100$ mm is a consequence of a decrease in the relative contribution of the direct electron-impact excitation from the ground state, and the large errors are due to the steep gradient of C_{14} at small T_e.

Another possible factor that could affect T_e and n_e is the effect of suprathermal electrons. If we approximate the electron velocity distribution as a weighted sum of two Maxwellian distributions, $C_{qp}(T_e)$ can be written as

$$C'_{qp}(T_{el}, T_{eh}) = (1 - \alpha)C_{qp}(T_{el}) + \alpha C_{qp}(T_{eh}), \qquad (4)$$

where T_{el} and T_{eh} ($T_{el} < T_{eh}$) represent the temperatures of the two distributions and α is the fraction of the high-temperature component. In this case, we confirmed that T_e determined by the fitting becomes approximately a weighted average of the two temperatures, $T_{e(avg)} = (1 - \alpha)T_{el} + \alpha T_{eh}$. If we assume a single electron temperature in the analysis, the excitation rate coefficient will be overestimated. This is because $C_{qp}(T_e)$ is a convex upward function, as schematically shown in the inset of Fig. 5, and $C'_{qp}(T_{el}, T_{eh}) < C_{qp}(T_{e(avg)})$. This primarily appears as an underestimation of n_{1^1S}. Figure 5 shows the calculated n_p in the cases of two temperatures and one temperature. The relative densities are similar but the absolute densities are smaller in the case of two temperatures. In particular, when $T_{el} < 5$ eV, errors in the estimated T_e and n_{1^1S} increase owing to the steep gradient of $C_{qp}(T_e)$.[27] Note that the detailed evaluation of the shape of the electron velocity distribution only using HeI line intensities is difficult, for which other diagnostics are required.[28] In the present ECR device, suprathermal electrons were found to exist locally around the ECR layer at 67 mPa;[29] thus, n_{1^1S} in this region may have been underestimated.

Finally, we comment on the number of emission lines required for the measurement. In the above analysis, we separated the HeII and 2^3P–4^3S lines as shown in Fig. 2. However, this separation may be impossible when the wavelength resolution of the adopted spectrometer is degraded. We thus attempted the above analysis while excluding the 4^3S state and found that the change in T_e from the values in Fig. 4 was less than 40%. Another possible procedure is to use only $n = 3$ states and omit Λ_{4^1P} from the fitting. For a high-density plasma, it was reported that this simplification does not significantly change the result,[2] and we found that this is also true for the present low-density case. Since the number of observed emission lines was six, we carried out the fitting using the QSS approximation for the 2^1S state to reduce the number of fitting parameters to five so as to evaluate the fitting errors. The determined parameters were found to agree with those in Fig. 4 within a factor of two.

In conclusion, from the practical viewpoint of applying the HeI line-intensity ratio method to low-density plasmas, we showed that it is necessary to set T_e, n_e, Λ, n_{1^1S}, n_{2^1S}, and n_{2^3S} as unknown variables and determine them

simultaneously by fitting. The omission of the OEFs and the application of the QSS approximation to the 2^3S metastable state cause a significant error in T_e and a smaller error in n_e. We also demonstrated that the method can be used to evaluate the transport of 2^3S metastable atoms and the depletion of ground-state atoms.

[1] O. Schmitz, I. L. Beigman, L. A. Vainshtein, B. Schweer, M. Kantor, A. Pospieszczyk, Y. Xu, M. Krychowiak, M. Lehnen, U. Samm, and B. Unterberg, and the TEXTOR Team, Plasma Phys. Controlled Fusion **50**, 115004 (2008).

[2] S. Kajita and N. Ohno, Rev. Sci. Instrum. **82**, 023501 (2011).

[3] K. Sawada, M. Goto, and N. Ezumi, Plasma Fusion Res. **6**, 1401010 (2011).

[4] Y. Iida, S. Kado, and S. Tanaka, J. Nucl. Mater. **438**, S1237 (2013).

[5] E. M. Hollmann, C. Brandt, B. Hudson, D. Kumar, D. Nishijima, and A. Yu. Pigarov, Phys. Plasmas **20**, 093303 (2013).

[6] M. Goto and K. Sawada, J. Quant. Spectrosc. Radiat. Transfer **137**, 23 (2014).

[7] W. Lee, K. Park, D.-H. Kwon, and C.-H. Oh, Phys. Plasmas **23**, 063516 (2016).

[8] S. Nowak, T. Pfau, and J. Mlynek, Appl. Phys. B **63**, 203 (1996).

[9] C. S. Allred, J. Reeves, C. Corder, and H. Metcalf, J. Appl. Phys. **107**, 033116 (2010).

[10] M. Kurahashi and Y. Yamauchi, Phys. Rev. Lett. **84**, 4725 (2000).

[11] W. M. Lytle, D. Andruczyk, and D. N. Ruzic, J. Vac. Sci. Technol. B **31**, 011603 (2013).

[12] A. Ueda, T. Shikama, T. Teramoto, T. Higashi, Y. Iida, and M. Hasuo, Appl. Phys. Lett. **111**, 074101 (2017).

[13] A. Fruchtman, J. Phys. D: Appl. Phys. **50**, 473002 (2017).

[14] K. Nagaoka, A. Okamoto, S. Yoshimura, M. Kono, and M. Y. Tanaka, Phys. Rev. Lett. **89**, 075001 (2002).

[15] F. E. Irons, J. Quant. Spectrosc. Radiat. Transfer **22**, 1 (1979).

[16] A. Molish and B. Oehry, *Radiation Trapping in Atomic Vapors* (Clarendon Press, Oxford, 1998).

[17] Y. Iida, S. Kado, and S. Tanaka, Phys. Plasmas **17**, 123301 (2010).

[18] T. Fujimoto, *Plasma Spectroscopy* (Clarendon Press, Oxford, 2004), Chap. 4.

[19] B. Schweer, G. Mank, and A. Pospieszczyk, J. Nucl. Mater. **196–198**, 174 (1992).

[20] M. Goto, J. Quant. Spectrosc. Radiat. Transfer **76**, 331 (2003).

[21] M. D. Kilgore, H. M. Wu, and D. B. Graves, J. Vac. Sci. Technol. B **12**, 494 (1994).

[22] P.-W. Lee and H.-Y. Chung, Phys. Lett. A **213**, 186 (1996).

[23] J. R. Taylor, *Introduction to Error Analysis: The Study of Uncertainties in Physical Measurements* (University Science Books, 1997), Sec. 12.3.

[24] K. Deguchi, T. Imagawa, T. Shikama, and M. Hasuo, J. Phys. B: At. Mol. Opt. Phys. **42**, 055403 (2009).

[25] T. Shikama, S. Ogane, Y. Iida, and M. Hasuo, J. Phys. D: Appl. Phys. **49**, 025206 (2016).

[26] See Ref. 18, Chap. 5B.

[27] S. Sasaki, S. Takamura, S. Watanabe, S. Masuzaki, T. Kato, and K. Kadota, Rev. Sci. Instrum. **67**, 3521 (1996).

[28] S. Coda, Rev. Sci. Instrum. **79**, 10F501 (2008).

[29] T. Teramoto, T. Shikama, A. Ueda, and M. Hasuo, "Detection of anisotropy in the electron velocity distribution produced by electron cyclotron resonance heating using the polarization of helium atom emission lines," Appl. Phys. Lett. (to be published).